Published in final edited form as:
Clin Exp Metastasis. 2011 August ; 28(6): 515–527. doi:10.1007/s10585-011-9388-6.

Mena invasive (Mena^{INV}) and Mena11a isoforms play distinct roles in breast cancer cell cohesion and association with TMEM

Evanthia T. Roussos[1], **Sumanta Goswami**[1,4], **Michele Balsamo**[3], **Yarong Wang**[1], **Robert Stobezki**[4], **Esther Adler**[7], **Brian D. Robinson**[5], **Joan G. Jones**[6], **Frank B. Gertler**[3], **John S. Condeelis**[1,2], and **Maja H. Oktay**[7]

[1]Department of Anatomy and Structural Biology, Albert Einstein College of Medicine, Bronx, NY 10461

[2]Gruss Lipper Biophotonics Center, Albert Einstein College of Medicine, Bronx, NY 10461

[3]David H Koch Institute for Integrative Cancer Research, Massachusetts Institute of Technology, Cambridge, MA 02139

[4]Department of Biology, Yeshiva University, New York, NY 10033

[5]Department of Pathology, Johns Hopkins Hospital, Baltimore, MD 21287

[6]Department of Pathology and Laboratory Medicine, Weill Cornell Medical College, New York, NY 10065

[7]Department of Pathology, Montefiore Medical Center, Bronx, NY 10467

Abstract

Mena, an actin regulatory protein, functions at the convergence of motility pathways that drive breast cancer cell invasion and migration *in vivo*. The tumor microenvironment spontaneously induces both increased expression of the Mena^{INV} and decreased expression of Mena11a isoforms in invasive and migratory tumor cells. Tumor cells with this Mena expression pattern participate with macrophages in migration and intravasation in mouse mammary tumors *in vivo*. Consistent with these findings, anatomical sites containing tumor cells with high levels of Mena expression associated with perivascular macrophages were identified in human invasive ductal breast carcinomas and called TMEM. The number of TMEM sites positively correlated with the development of distant metastasis in humans. Here we demonstrate that mouse mammary tumors generated from EGFP-Mena^{INV} expressing tumor cells are significantly less cohesive and have discontinuous cell-cell contacts compared to Mena11a xenografts. Using the mouse PyMT model we show that metastatic mammary tumors express 8.7 fold more total Mena and 7.5 fold more Mena^{INV} mRNA than early non-metastatic ones. Furthermore, Mena^{INV} expression in fine needle aspiration biopsy (FNA) samples of human invasive ductal carcinomas correlate with TMEM score while Mena11a does not. These results suggest that Mena^{INV} is the isoform associated with breast cancer cell discohesion, invasion and intravasation in mice and in humans. They also imply that Mena^{INV} expression and TMEM score measure related aspects of a common tumor cell dissemination mechanism and provide new insight into metastatic risk.

Correspondence: Evanthia T. Roussos evanthia.roussos@med.einstein.yu.edu, (718) 678-1131, John Condeelis john.condeelis@einstein.yu.edu, Maja H. Oktay, (718) 920-6091,moktay@montefiore.org.
Evanthia T. Roussos (evanthia.roussos@med.einstein.yu.edu), Sumanta Goswami (sumanta.goswami@einstein.yu.edu), Michele Balsamo (mbalsamo@mit.edu), Yarong Wang (yarong.wang@einstein.yu.edu), Robert Stobezki (stobezki@yu.edu), Esther Adler (eadler@montefiore.org), Brian D. Robinson (brr2006@nyp.org), Joan G. Jones (joj2013@med.cornell.edu), Frank B. Gertler (fgertler@mit.edu), John S. Condeelis (john.condeelis@einstein.yu.edu), Maja H. Oktay (moktay@montefiore.org)

Keywords

Breast cancer; metastasis; cell motility; intravasation; TMEM

INTRODUCTION

Multiphoton-based intravital imaging has demonstrated that invasive carcinoma cells in mouse and rat mammary tumors migrate and intravasate when associated with migratory [1] and peri-vascular macrophages [2], respectively. An *in vivo* invasion assay has been used in mammary tumors of rats, mice, and humans to collect migratory tumor cells associated with macrophages and these cells have been expression profiled [3]. The gene expression changes occurring in migratory and macrophage-associated tumor cells are clustered in several pathways including the motility pathways regulating EGF stimulated locomotion. Many of these genes belong to the "minimum motility machine" comprised of the cofilin/LIM kinase, N-WASP/Arp2/3 complex and Mena/capping protein pathways [4-6]. Several genes that coordinate and control the activity of these pathways are also up regulated. One of these genes is Mena. Mena protein promotes actin polymerization by interfering with the activity of inhibitory capping proteins [7]. The anti-capping function of Mena promotes sustained actin polymerization, which is essential for directional cell movement in response to growth factors like EGF.

Mena is upregulated in rat, mouse and human mammary tumors [8-10]. Similarly, in precursor lesions to cancer of the cervix and colon, Mena expression is increased with progressive transformation [11, 12]. Mena has been used successfully as part of a marker of metastatic risk called TMEM (Tumor Micro-Environment of Metastasis) observed in formalin-fixed paraffin-embedded sections of human invasive ductal carcinomas of the breast [9]. TMEM is an anatomical site consisting of a macrophage in direct contact with a Mena expressing tumor cell, and an endothelial cell. TMEM counts are associated with risk of metastasis in breast cancer patients independently of lymph node, ER/PR or HER2 status [9].

Mena, a member of the Ena/VASP family of proteins, regulates membrane protrusion and cell movement in a variety of cell types and contexts by influencing the geometry and assembly of actin filament networks [13-17]. Mena is alternatively spliced. In particular, an exon encoding a sequence of 19 amino acids inserted between the EVH1 domain and the LERER repeats generates a Mena invasion (^{INV}) isoform (previously called Mena^{+++}) [13, 18] and inclusion of an exon encoding a 21 amino acid insertion in the EVH2 domain produces the Mena11a isoform [6]. Until recently, Mena^{INV} was thought to be expressed primarily in axons of developing neurons [13], wheras expression of Mena11a was found in epithelial cancer cells [6]. However, expression profiling of cells collected using the *in vivo* invasion assay revealed that Mena^{INV} expression is specifically upregulated and Mena11a is downregulated in migratory/macrophage associated tumor cells compared to average primary tumor cells (APTCs) isolated from the same rat and mouse mammary tumors by FACS [8]. Expression of Mena^{INV} in a xenograft mouse model increases spontaneous lung metastases from mammary tumors and alters the dose-response of tumor cells to epidermal growth factor (EGF), allowing cells to respond to much lower EGF concentrations than control cells both *in vivo* and *in vitro* [17].

Here we demonstrate that Mena^{INV} promotes discohesive tumor morphology in a xenograft mouse model while Mena11a expression promotes cohesive tumor morphology. We also show that increased expression of Mena^{INV} but not Mena11a is associated with metastasis in the PyMT mouse model of breast cancer. Furthermore, we demonstrate that Mena^{INV}

expression correlates with the assembly of cancer cell intravasation sites in human breast cancers using TMEM score. It seems that both TMEM score and Mena isoform expression measure an aspect of tumor biology unrelated to standard clinical and pathological parameters because they do not correlate with tumor, size, lymph node status or ER, PR and HER2/Neu receptor expression. Thus, we suggest that Mena^{INV} may have useful clinical applications as a prognostic marker for metastatic risk and target for therapy.

MATERIALS AND METHODS

Cell lines, molecular cloning, infection, fluorescence-activated cell sorting and cell culture

EGFP-Mena splice isoforms were subcloned into the retroviral vector packaging Murine stem cell virus-EGFP using standard techniques [14]. MTLn3 rat adenocarcinoma cells were infected with each Mena isoform construct to create MTLn3-EGFP-Mena (referred to as Mena cells), MTLn3-EGFP-Mena^{INV} (referred to as Mena^{INV} cells) and MTLn3-EGFP-Mena11a cells (referred to as Mena11a cells) and used for all orthotopic injections of SCID mice. Details about the retroviral system used to generate these lines have been described previously [17]. Monoclonal MTLn3 cells were derived from spontaneous lung metastases in a rat model 13762 [19], and were used in these experiments because they are known to metastasize to the lung when injected into the mammary gland of SCID mice and thus are suitable for metastatic studies [20]. Additionally, these cells have been used to study Mena isoforms previously [17, 21]; thus we wished to be able to compare current work with work previously published. To achieve uniform forced expression, EGFP -Mena^{INV} and -Mena11a cells were FAC sorted to a level of 4-fold overexpression of EGFP-Mena isoforms as compared to EGFP-Mena on the protein level. MTLn3-Cerulean EGFP-Mena splice isoforms were created using a lentiviral system pCCLsin.PPT.hPGK.Cerulean.pre (courtesy of Dr. Gupta, Albert Einstein College of Medicine). Cytoplasmic expression of Cerulean was used to improve visualization of tumor cells during intravital imaging. MTLn3 cells were cultured in alpha-modified minimum essential medium (MEM) supplemented with 5% fetal bovine serum (FBS) and 0.5% PenStrep (Invitrogen).

Xenograft animal models

Orthotopic mammary tumors were derived by the subcutaneous injection of 1×10^6 EGFP-MTLn3 (referred to as GFP), -EGFP-Mena, -EGFP-Mena^{INV} -EGFP-Mena11a, -Cerulean-EGFP-Mena^{INV} or - Cerulean-EGFP-Mena11a cells into the mammary gland of 5–7 week-old female SCID mice (these mice are referred to as xenograft mice) [22]. All experiments involving animals were approved by the Einstein Institute for Animal Studies.

Intravital Imaging (IVI)

Intravital multiphoton imaging was performed in tumors of SCID mice expressing MTLn3-cerulean-EGFP-Mena^{INV} or cerulean-EGFP-Mena11a as described previously [23, 24] using a 20× 1.95 NA water immersion objective with correction lens. Briefly, a skin flap surgery was performed to expose the mammary tumor of an anesthetized mouse and the mouse was then placed on the microscope for imaging. Visualization of collagen within the primary tumor is made possible by the generation of a second harmonic signal which results from the reflection of light off of collagen helices [25].

Scoring of cohesive and discohesive tumor morphology was done using images obtained with intravital multiphoton microscopy. A minimum of 4 fields from each tumor imaged in xenograft mice were divided into quadrants. 5 mice per isoform type were evaluated (a total of 20 fields were scored per tumor type). A score of C (cohesive) indicated a quadrant containing a continuous sheet/ large cluster of tumor cells. A score of D (discohesive) indicated that > ½ of the quadrant lacked continuous sheets or clusters of cells. Data in

figure 1d is represented as percentage of total fields analyzed that received a score of C versus percentage of fields that received a score of D. Images were scored double blind and the findings from each correlated with each other.

Fine Needle Aspiration (FNA) of MTLn3 Xenografts

Mice were euthanized 3 weeks after carcinoma cell injection into the mammary gland. FNA was performed as previously described [26]. In brief, cells collected with 25 gauge needles were expelled onto a glass slide and smeared. Smears were stained by standard Diff-Quick protocol [26]. Each smear was given a score based on the ratio of the number of clusters to the approximate percentage of single cells, either <30% <60% or <90% as observed in a single low power field area (40X; 12.56 mm^2). A cluster was defined as >10 cells in direct contact with each other. Each smear was also independently described as cohesive or discohesive based on the relative abundance of clusters as compared to single cells. Both methods were scored double blind and the findings from each correlated with each other.

Real Time PCR

PCR analyses were performed using SyBR Green kit and ABI 7300 sequence detector. Primers detected $Mena^{INV}$ and Mena11a as described previously [8]. The data were analyzed by ABI Sequence Detection Software (Applied Biosystems Foster City, CA).

Immunofluorescence (IF) and immunohistochemistry (IHC)

Following 4 weeks of tumor growth, five primary tumors from xenografts of each tumor type derived from injection of MTLn3-EGFP, -EGFP-Mena, -EGFP-Mena11a and –EGFP-$Mena^{INV}$, cells were fixed in 10% buffered formalin and paraffin embedded. Sections 10βm thick were cut from each tumor and placed on slides for further staining. IF was done using anti-GFP (Aves Lab Cat. #1020) at 1:500 dilution with Alexa488 as a secondary, and anti-β-catenin (BD Biosciences Cat. #610153) at 1:500 dilution with Alexa594 as a secondary. Digital images were converted in ImageJ (NIH) and analyzed using macro analysis that defines fluorescence intensity starting at the cell periphery and extend into the cell interior [27]. Primary tumor sections were imaged using the Zeiss AxioObserver.Z1 with a 10× 1.4 NA Plan Apo objective with the apotome and processed using ImageJ (NIH).

IHC for E-cadherin was done using commercially available monoclonal anti-E cadherin antibody (Dako, Carpinteria, CA) at 1:25 dilution. Antigen retrieval was done in a steamer at 90°C for 30 minutes in Target Retrieval solution pH 6.0. The slides were incubated with the primary antibody for 30 minutes at room temperature and 30 minutes with a secondary antibody. E-cadherin was visualized using anti-mouse horseradish peroxidase-labeled polymer (Envision System, Dako) and DAB on an automated immunostainer (Autostainer, Dako) according to the manufacturer's instructions. The slides were counterstained with hematoxylin using standard technique.

Western Blots

MTLn3 protein lysates were prepared, the samples were resolved by SDS-PAGE, transferred to nitrocellulose, blocked in odyssey blocking solution (LiCor), incubated in primary antibodies overnight at 4°C, secondary antibodies for 1 hour at room temperature, and analyzed using the Odyssey (LiCor) [28]. Primary antibodies, anti-Mena [1:1000] [29], anti-Mena11a [1:5000] [30], anti-$Mena^{INV}$ [1:500] (unpublished, more information available upon request), anti-beta-actin [1:5000] (Invitrogen), were used at the indicated concentrations. Secondary antibodies, Mouse 680 (used against actin and Mena) and Rabbit 800 (used against Mena11a and $Mena^{INV}$) were purchased from LiCor and imaged in

separate channels. Endogenous Mena, Mena11a and Mena^{INV} were detected at lower molecular weights as compared to EGFP-Mena11a and EGFP-Mena^{INV}.

Collection and Processing of Polyoma Middle T Antigen Induced Mouse Mammary Tumors

Transgenic animals with mammary gland-specific expression of Polyoma middle T (PyMT) antigen in the FVB-C3H/B6 background were obtained from the Albert Einstein College of Medicine mouse repository. FNA was performed with a 25 gauge needle on animals anesthetized with 5% isoflurane and sacrificed by cervical dislocation. The initial FNA biopsy was used for quality assessment using standard Diff-Quick stain. Subsequent biopsies were used for qRT-PCR analysis. Staging of H&E stained tumor sections from formalin fixed, paraffin embedded tissue was done as previously described [31].

Human Tissue Selection and FNA Biopsy Procedure

Lumpectomy and mastectomy specimens received at the Albert Einstein College of Medicine/ Montefiore Medical Center, Moses and Weiler Divisions for pathological examination were used for FNA-based tissue collection under institutional IRB approval. Four to five FNA aspiration biopsies were performed on grossly visible lesions using 25 gauge needles. The adequacy of the sample was assessed by standard Diff-Quick protocol [26]. Only samples composed of 90% of either benign or malignant epithelial cells, as determined by standard pathologic characteristics [26], were used in the study.

Tissue Selection for TMEM staining, TMEM staining and scoring

At the time of routine microscopic examination of the lesions on which FNA biopsies had been performed, an appropriate area of the tumor suitable for TMEM analysis was identified by low power scanning. The following criteria were used: high density of tumor, adequacy of tumor, lack of necrosis or inflammation, and lack of artifacts such as retraction or folds. TMEM staining and assessment were done as described previously [9]. Briefly, ten digital images were acquired at 400x total magnification. Using the “circle” tool available in Photoshop, all TMEM are “marked” using circles, and the “marked” images are saved as separate files. The total TMEM count for each image was tabulated, and the counts from all ten images are then summed to give a final TMEM density for each patient sample, expressed as the number of TMEM per 10 high power fields (400x total magnification). Two pathologists independently scored all fields. The scores for each case were averaged for the two pathologists to yield a final score used in the data analysis.

E-Cadherin scoring

Similarly to TMEM scoring, ten digital images were acquired at 400x total magnification for each xenograft tumor and cells with complete membranous staining were marked with asterisk using Photoshop tools. The total number of cells from all ten images was summed to give a final number of cells with complete E-cadherin membranous stain for each xenograft. There were 3 xenografts per group; thus a total of 30 high power fields (400x total magnification) were analyzed per group. The results are expressed as a mean (with SEM) of number of cells with complete membranous stain per group.

Relationship of FNA Sample to TMEM

FNA primarily collects loose tumor cells with very few macrophages and no endothelial cells and incurs minimal tissue damage [32]. Thus, after the FNA procedure, the entire tumor was formalin-fixed, paraffin-embedded (FFPE) and sent for pathological examination. A representative block of FFPE tumor tissue was selected and triple immunostained for TMEMs. Therefore, the FNA sample and TMEM count were obtained from the same tumor for the entire cohort (Figure S3).

Statistical Analysis

Statistical significances were determined using unpaired, two-tailed Student's t-tests assuming equal variances and an alpha level of 0.05. Differences were considered significant if the p value was <0.05. Actual P-values are listed on graphs within each figure. For differences in Mena isoform expression between metastatic and non-metastatic PyMT tumors and the association between TMEM density or Mena isoform fold change with tumor grade, lymph node status, tumor size, ER, PR and Her2/Neu status, Wilcoxon Mann-Whitney rank-sum test was used. Given that 6 comparisons were done for human samples, the P values for determining statistical significance was set at 0.008 by applying the Bonferroni correction to the standard assumption that $P < 0.05$ is statistically significant. The strength of association between Mena isoform expression and TMEM density was calculated using Spearman's correlation coefficient.

RESULTS

Expression of Mena11a, but not Mena^{INV} promotes cohesive primary tumor morphology and integrity of cell-cell junctions

To investigate the effects of expression of Mena, Mena^{INV} and Mena11a on primary tumor morphology and tumor cell cohesiveness, we generated orthotopic mammary tumors from MTLn3 rat adenocarcinoma cell lines forced to express Mena, Mena^{INV} and Mena11a isoforms. Our previous studies show that invasive tumor cells spontaneously increase expression of Mena^{INV}, and decrease expression of Mena 11a *in vivo* [8]. We also showed that MTLn3 mammary carcinoma cells forced to express Mena^{INV}, are sensitized to EGF and are more metastatic [17]. We hypothesized that the highly invasive and metastatic nature of Mena^{INV} cells might be in part caused by decreased tumor cell cohesion [6, 33]. Likewise, the expression of Mena 11a, characteristically found in more epithelial tumor cells [6] and non invasive tumor cells *in vivo* [8], might promote cohesive tumor cell morphology. These considerations also suggest that FNA of tumors could be used to detect differences in Mena expression patterns. To test this, FNA samples were collected from MTLn3-derived mammary tumors. Examples of cohesive and discohesive FNA cytopathology smear patterns are shown in Figure 1a. We found that FNA smears obtained from Mena11a expressing mammary tumors were more cohesive than smears obtained from Mena and Mena^{INV} expressing mammary tumors (Figure 1b). MTLn3 control tumors (referred to as GFP) and tumors derived from Mena and Mena^{INV} expressing MTLn3 cells had similar discohesive smear patterns (Figure 1b). Quantification of cell clusters and discohesive areas confirmed that Mena11a tumors were significantly more cohesive than GFP, Mena or Mena^{INV} tumors (Figure 1b).

To further characterize the effects of Mena, Mena11a and Mena^{INV} on tumor cell cohesion within the primary tumor we used multiphoton-based intravital imaging (IVI). Within the intact primary tumor of an anesthetized mouse, Mena11a expressing tumors had well defined cohesive cell-cell contacts, whereas Mena^{INV} expressing tumors had discontinuous cell-cell contacts and the cells were more randomly organized resulting in a discohesive appearance (Figure 1c, S1). Mena expressing tumors also demonstrated more discohesive appearance as compared to GFP tumors but did not show as drastic a trend toward discohesion as that seen in Mena^{INV} expressing tumors. All images were taken under non-bleached conditions with lower laser power of the multiphoton microscope allowing the weaker cytoplasmic fluorescence to persist. This allowed direct comparison of Mena, Mena^{INV}, and Mena11a expressing tumor cells and demonstrates that Mena is more diffuse than the Mena11a or Mena^{INV} isoforms (Figure 1c).

Primary tumor morphologies were scored based on cohesive and discohesive appearance in tumors expressing GFP fused to the Mena isoform indicated. Mena11a tumors had the largest percentage of cohesive fields while Mena^{INV} tumors had the largest percentage of discohesive fields (Figure 1d).

Given the strong correlation of Mena11a expression with cohesion, and Mena^{INV} expression with discohesion of tumor cells, we asked whether Mena^{INV} and Mena11a isoform expression affects the integrity of cell-cell junctions using β-catenin and E-cadherin immunofluorescence and immunohistochemistry, respectively. Localization of these proteins at cell-cell contacts has been used to investigate cell junction integrity [34, 35]. Mena11a expressing mammary tumors exhibited continuous β-catenin immunofluorescence staining at cell-cell contacts while staining for β-catenin in Mena^{INV} expressing mammary tumors was discontinuous (Figure 2a). Mena11a tumor cells also had a significantly higher intensity of β-catenin staining at cell-cell contacts (Figure 2b), and within the whole cell (Figure S2) as compared to Mena^{INV} cells. Mena expressing tumor cells had similar localization of β-catenin at cell-cell contacts (Figure 2a) and increased expression within the whole cell (Figure S2) as compared to GFP control tumors. In addition to a reduction in β-catenin staining, tumor cells from Mena^{INV} expressing tumors also showed a dramatic reduction in continuous E-cadherin staining at cell-cell junctions as compared to that seen in GFP and Mena11a expressing tumors (Figure 2c). E-cadherin staining pattern was similar to β–catenin; predominantly discontinuous in Mena^{INV} tumors when compared to GFP, Mena or Mena11a expressing tumors (Figure 2c and d). We found significantly lower numbers of cells with complete membranous staining in Mena^{INV} tumors than in GFP control, Mena or Mena11a expressing tumors (Figure 2d), consistent with our finding that Mena11a promotes a cohesive epithelial morphology while Mena^{INV} supports a discohesive morphology *in vivo*.

To rule out if the observed effects of Mena^{INV} and Mena11a cells on invasion are due to compensatory expression of the different Mena isoforms we performed western blots on each cell line to check for expression of each Mena isoform. In Mena^{INV} cells the levels of endogenous Mena or Mena11a were unchanged as compared to GFP control cells (Figure 3). In Mena11a there were no detectable differences in Mena or Mena^{INV} levels as compared to GFP cells (Figure 3).

The expression level of Mena, Mena^{INV} and Mena11a isoform mRNA correlates with cell cohesiveness, and metastatic status in PyMT oncogene induced mouse mammary carcinomas

To assess how cohesion and Mena isoform expression correlate with metastatic status we studied PyMT mouse mammary carcinoma. These tumors histologically recapitulate progression of human ductal carcinoma of the breast from ductal hyperplasia and ductal carcinoma *in situ* to invasive ductal carcinoma [31]. Invasive ductal carcinomas in PyMT tumors can be additionally stratified into histologically distinct subcategories of early and late carcinomas. Unlike in humans where cancer morphology does not reflect tumor metastatic potential, late PyMT cancers are associated with tumor cell dissemination and lung metastases [31, 36, 37]. Thus we assessed the FNA smear pattern and Mena isoform expression in early and late PyMT tumors to determine if Mena isoform mRNA expression correlates with the smear pattern and metastatic outcome. Smear patterns obtained from early PyMT mouse mammary tumors were predominantly cohesive, while those obtained from late, metastatic tumors were predominantly discohesive (Figure 4a-i and 4a-ii). Quantitative real time PCR (qRT-PCR) of FNA samples shows a spontaneous 8.7-fold increase in pan-Mena expression (determined with primers that identify all Mena isoforms = pan-Mena) and 7.5-fold increase in Mena^{INV} expression in late carcinomas when compared with early carcinoma, while Mena11a amplicons were decreased by 70% in late carcinomas

(Figure 4b). Thus, the Mena isoform expression pattern in cells collected by FNA from late, metastatic tumors matches that of the invasive cells collected by the *in vivo* invasion assay while the Mena expression pattern from early carcinomas matches that of average primary tumor cells (APTCs) isolated from the same rat and mouse mammary tumors by FACS (2). This finding suggests that the pattern of Mena isoform expression in FNA samples may reflect invasive potential of FNA collected cancer cells.

Mena^{INV} isoform mRNA expression correlates with the TMEM intravasation score and metastatic risk in human invasive ductal carcinomas of the breast

The correlation of spontaneously increased Mena^{INV} and decreased Mena11a expression with tumor progression and metastatic outcome in transgenic PyMT mouse mammary tumors, and our recent findings showing that Mena^{INV}, but not Mena11a, expression increases tumor cell motility, intravasation and dissemination in xenograft mouse mammary tumors [17, 21], led us to ask if the altered expression of these isoforms correlates with an increased risk of metastasis in humans.

Since our study is prospective we used TMEM score as a measure of increased metastatic risk. As previously shown TMEMs are visualized by a triple immunostain to detect the direct contact of macrophages, Mena expressing carcinoma cells and endothelial cells in formalin fixed paraffin embedded tissues [9]. The number of TMEM sites has been shown previously to be significantly higher in tumors that produce distant metastases [9]. TMEM was developed based on studies that used multiphoton intravital imaging of mammary tumors in PyMT mice showing breast carcinoma cells intravasating at sites along blood vessels where peri-vascular macrophages are in direct contact with tumor cells and endothelial cells [38, 39]. Examples of TMEMs (marked by circles) are shown in two human invasive ductal carcinomas as identified in histological sections (Figure 5a). TMEM was also identified in xenograft mammary tumors derived from injection of MTLn3-Mena^{INV} cells (Figure 5b).

We hypothesize that Mena^{INV} expressing tumor cells are involved in the assembly of TMEM and therefore human tumors with numerous TMEM intravasation sites will have a higher proportion of discohesive, invasive and migratory tumor cells expressing Mena^{INV} compared to tumors with few TMEM sites. To investigate this we collected cells from 40 patients' invasive ductal carcinomas (IDC) and 5 fibroadenomas by FNA.

The expression of Mena, Mena11a and Mena^{INV} at the protein level was assessed by western blotting. As shown in 4 randomly chosen FNA samples (Figure S4), Mena isoform expression is detectable at the protein level, but only with long exposure. While these blots establish that the Mena isoforms are expressed at the protein level in FNA samples, the number of cells collected in FNA samples was variable and not sufficient for western blot analysis of correlations with TMEM count. Thus, the quantification of Mena isoform expression was determined by PCR for all FNA samples to be correlated with TMEM count.

Therefore, PCR primers specific to the Mena isoforms of interest were used with all 40 FNA samples and the results were expressed as a fold change of Mena isoform mRNA expression in IDC, compared to the mean level of Mena isoforms mRNA obtained from 5 fibroadenomas. TMEM counts were scored in tumor samples obtained from the same cohort of 40 patients, and were correlated with the fold change in Mena isoform mRNA expression (Figure 5c). The tissue collection methods are outlined in Figure S3. The Spearman's correlation coefficient for the association between Mena^{INV} fold change and TMEM count was 0.78 ($p= 10^{-6}$). An inverse association between Mena11a and TMEM was also expected but was not found ($r = -0.23$, $p= 0.14$).

We also evaluated the collective fold change of all Mena isoforms using primers that amplify all Mena isoforms (pan-Mena). The expression of pan-Mena did not correlate with TMEM score ($r = -0.15$, $p = 0.37$) (Figure 6). These results indicate that Mena^{INV} is the isoform that is correlated with TMEM count and therefore with the metastatic risk in breast carcinoma.

These same tumor samples were also classified according to the modified Bloom Richardson scale. Patients' age, tumor size, tumor grade, lymph node status, estrogen, progesterone and HER2/Neu receptor status were documented along with Mena^{INV}, Mena11a expression level and TMEM score (Table S1). Median values as well as 5th and 95th percentiles of Mena^{INV}, Mena11a expression levels and TMEM scores for all recorded tumor characteristics stated above was calculated (Table 1). We found statistically significant difference in TMEM score between the tumors of low and high grade ($p = 0.004$). However, no statistically significant difference in Mena isoform mRNA fold change among the tumors of different grades was found. Likewise, there was no statistically significant difference in TMEM score and Mena isoform mRNA fold change among tumors of different size, lymph node status, ER, PR and HER2/Neu expression, suggesting that both TMEM score and Mena isoform mRNA expression reflect mechanisms of tumor invasion/progression independent of most currently used clinical and pathological parameters.

These data indicate that the expression of Mena^{INV} mRNA correlates with TMEM score, and are consistent with the PyMT mouse tumor results showing that expression of Mena^{INV}, but not Mena11a, correlates with metastasis (Figure 4b). They are also consistent with the results of our recent xenograft experiments documenting that Mena^{INV} is the isoform associated with increased intravasation, dissemination and higher rates of lung metastasis [21].

DISCUSSION

Animal models indicate that carcinoma cells located in invasion-inducing microenvironments undergo transient and sometimes stable epigenetic changes similar to those that drive morphogenetic cell movements in the developing embryonic organ [2, 40-42]. One of the changes is the increased expression of the actin regulatory protein Mena^{INV} and decreased expression of Mena11a [8]. Here we have found that changes in isoform expression from Mena11a to Mena^{INV} correlate with the loss of epithelial cell-cell contacts and the emergence of a discohesive cell population in the primary tumor. Additionally, previous studies have reported an increase in cell motility *in vivo* and lung metastases in orthotopic mammary tumors derived from Mena^{INV} expressing tumor cells [17]. Thus, the discohesive primary tumor morphology and discontinuous cell-cell adhesion contacts observed in Mena^{INV} tumors supports the enhanced migratory phenotype previously reported [17].

We demonstrate that expression of Mena11a promotes the maintenance of epithelial cell-cell contacts and a cohesive cell population within a mammary tumor. This is consistent with recent findings showing that expression of Mena11a delays but does not prevent metastatic progression in MTLn3 xenograft mammary tumors [21]. These results suggest that the expression of Mena11a in tumor cells will support their retention in cohesive regions of tissue with relatively stable cell-cell junctions (Figure 7). Thus, the FNA smears from the tumors with the high proportion of Mena11a expressing cells show mostly cohesive clusters likely reflecting a less malignant clinical outcome.

Previous studies have shown that Mena^{INV} expressing carcinoma cells have increased movement *in vivo* [17] (Figure 7-Box i). Sensitivity of tumor cells to a particular

chemoattractant will determine the direction and speed of their movement within the tissue [22]. Previous studies also show that Mena^{INV} expressing cells are hypersensitive to EGF during *in vivo* invasion [17]. This sensitivity could therefore promote migration toward, and association with EGF producing perivascular macrophages, resulting in intravasation (Figure 7-Box iii). This hypothesis is supported by previous observations of carcinoma cell migration toward blood vessels and intravasation in mouse mammary tumors [39]. We propose that a high proportion of single cells in FNA smears, and their expression of Mena^{INV}, is likely to reflect the presence of a migratory, and intravasation competent cell population, and therefore an adverse clinical outcome.

Our results show that the presence of Mena^{INV} expressing carcinoma cells in FNA samples is correlated with the presence of the anatomical structure called TMEM [9, 17]. As previously mentioned, TMEM is defined as the direct contact of a perivascular macrophage, an endothelial cell and Mena expressing tumor cell (Figure 7-Box ii). In recent findings we show that Mena^{INV} expressing carcinoma cells have dramatically increased intravasation [21]. Thus, it is possible that the expression of Mena^{INV} can provide an advantage to tumor cells in their ability to find macrophages when located in microenvironments with low concentrations of EGF due to the increased sensitivity of Mena^{INV} tumor cells to EGF [17]. These findings indicate that increased Mena^{INV} expression may affect metastatic potential of a particular breast tumor by contributing to macrophage-dependent cell motility throughout the primary tumor (Figure 7 Box i), and intravasation at TMEM sites (Figure 7-Box ii and iii). Indeed, our findings in PyMT mice indicate that Mena^{INV} promotes metastatic progression.

We show here that human invasive ductal carcinomas with high Mena^{INV} expression in FNA samples correlate with a high TMEM score. However, expression of Mena11a does not correlate with TMEM score and this is consistent with the recent findings that Mena11a expressing tumor cells have no effect on intravasation or metastasis relative to GFP control cells [21]. The observations in human tumors also suggest that expression of the Mena11a isoform does not affect the late stages of metastasis. These results support the involvement of the Mena^{INV} isoform in assembly of TMEM, and intravasation in human breast carcinomas.

We recently reported a case-control study demonstrating that TMEM density is associated with increased risk of metastasis of invasive ductal carcinomas of the breast [9]. That study demonstrated that TMEM count correlates with tumor grade supporting the fact that low grade tumors rarely metastasize. We also found a significant difference in TMEM score between low and high tumor grades in our cohort ($p= 0.004$). In both the previous and current studies, we did not observe any association between TMEM count and ER, PR, HER2/Neu expression or lymph node metastasis. Since about 10-15% of patients develop metastatic disease within 3 years of diagnosis [4, 5] we would expect about 5 cases from our cohort of 40 to be metastatic within the same time frame. Indeed, only 5 cases from our cohort (15%) have TMEM values around or above the 90th percentile (107.6) (Table S1 and Figure 5c). Three of those cases also have Mena^{INV} around or above the 90th percentile (5.64).

In summary, our results indicate that carcinoma cells with an elevated Mena^{INV} expression are discohesive (Figure 5 Box i), while those with elevated Mena11a expression are more cohesive. Our results also suggest that Mena^{INV} expressing cells assemble TMEM, and intravasate at TMEM sites (Figure 5 Box ii and iii). It will be important to determine how epigenetic changes may affect isoform expression and if these changes act through control of alternative splicing. Studies are underway to investigate the role of alternative splicing mechanisms in control of Mena isoform expression (FG, unpublished). Future studies will

investigate molecular and biochemical mechanisms of action of the Mena^{INV} and Mena11a isoforms, as well as their utility as predictors of breast cancer outcome and as targets for therapy.

Supplementary Material

Refer to Web version on PubMed Central for supplementary material.

Acknowledgments

We would like to thank Drs. Jeffery Segall, Diane Cox, Antonia Patsialou, and Daqian Sun for stimulating discussion and helpful suggestions. We also thank Drs. Sasis Sirikanjanapong, Jason Moss, and Zhong, as well as research associate Mrs. Felicia Juliano for assistance with FNA biopsy procedures, Dr. Jaya Sunkara for assistance with E-cadherin staining, and Dr. Olena Dorokhova for help with RNA extraction and cDNA synthesis. Many thanks to David Entenberg, and Jenny Tadros for their technical support, Einstein histopathology, Analytical Imaging Facilities, and Koch Institute for Microscopy, Histology and Flow Cytometry sorting core facilities for their services. Grant support provided by CA100324 (SG, YW), CA113395 (MHO, JSC), CA126511 (MHO, JSC), CA150344 (ETR), AECC9526-5267 (MHO, SG), Ludwig Fund postdoctoral fellowship (MB), GM58801 and funds from the Ludwig center at MIT (FBG), ICBP grant U54 CA112967 (FBG).

List of Abbreviations

EGF	epidermal growth factor
EGFP	enhanced green fluorescent protein
FACs	fluorescence activated cell sorting
FFPE	formalin-fixed paraffin-embedded
FNA	fine needle aspiration
IHC	immunohistochemistry
IF	immunofluorescence
IVI	intravital imaging
qRT-PCR	quantitative real time polymerase chain reaction
SCID	severe combined immunodeficiency
TMEM	tumor microenvironment for metastasis
APTC	average primary tumor cells

References

1. Sahai E, et al. Simultaneous imaging of GFP, CFP and collagen in tumors in vivo using multiphoton microscopy. BMC Biotechnol. 2005; 5:14. [PubMed: 15910685]
2. Condeelis J, Singer RH, Segall JE. The great escape: when cancer cells hijack the genes for chemotaxis and motility. Annu Rev Cell Dev Biol. 2005; 21:695–718. [PubMed: 16212512]
3. Wang W, et al. Identification and testing of a gene expression signature of invasive carcinoma cells within primary mammary tumors. Cancer Res. 2004; 64(23):8585–94. [PubMed: 15574765]
4. Heimann R, et al. Separating favorable from unfavorable prognostic markers in breast cancer: the role of E-cadherin. Cancer Res. 2000; 60(2):298–304. [PubMed: 10667580]
5. Weigelt B, Peterse JL, van 't Veer LJ. Breast cancer metastasis: markers and models. Nat Rev Cancer. 2005; 5(8):591–602. [PubMed: 16056258]
6. Di Modugno F, et al. Molecular cloning of hMena (ENAH) and its splice variant hMena+11a: epidermal growth factor increases their expression and stimulates hMena+11a phosphorylation in breast cancer cell lines. Cancer Res. 2007; 67(6):2657–65. [PubMed: 17363586]

7. Gertler F, Condeelis J. Metastasis: tumor cells becoming MENAcing. Trends Cell Biol. 2010
8. Goswami S, et al. Identification of invasion specific splice variants of the cytoskeletal protein Mena present in mammary tumor cells during invasion in vivo. Clin Exp Metastasis. 2009; 26(2):153–9. [PubMed: 18985426]
9. Robinson BD, et al. Tumor microenvironment of metastasis in human breast carcinoma: a potential prognostic marker linked to hematogenous dissemination. Clin Cancer Res. 2009; 15(7):2433–41. [PubMed: 19318480]
10. Di Modugno F, et al. The cytoskeleton regulatory protein hMena (ENAH) is overexpressed in human benign breast lesions with high risk of transformation and human epidermal growth factor receptor-2-positive/hormonal receptor-negative tumors. Clin Cancer Res. 2006; 12(5):1470–8. [PubMed: 16533770]
11. Gurzu S, et al. The expression of cytoskeleton regulatory protein Mena in colorectal lesions. Rom J Morphol Embryol. 2008; 49(3):345–9. [PubMed: 18758639]
12. Gurzu S, et al. The immunohistochemical aspects of protein Mena in cervical lesions. Rom J Morphol Embryol. 2009; 50(2):213–6. [PubMed: 19434313]
13. Gertler FB, et al. Mena, a relative of VASP and Drosophila Enabled, is implicated in the control of microfilament dynamics. Cell. 1996; 87(2):227–39. [PubMed: 8861907]
14. Bear JE, et al. Negative regulation of fibroblast motility by Ena/VASP proteins. Cell. 2000; 101(7): 717–28. [PubMed: 10892743]
15. Drees F, Gertler FB. Ena/VASP: proteins at the tip of the nervous system. Curr Opin Neurobiol. 2008; 18(1):53–9. [PubMed: 18508258]
16. Neel NF, et al. VASP is a CXCR2-interacting protein that regulates CXCR2-mediated polarization and chemotaxis. J Cell Sci. 2009; 122(Pt 11):1882–94. [PubMed: 19435808]
17. Philippar U, et al. A Mena invasion isoform potentiates EGF-induced carcinoma cell invasion and metastasis. Dev Cell. 2008; 15(6):813–28. [PubMed: 19081071]
18. Urbanelli L, et al. Characterization of human Enah gene. Biochim Biophys Acta. 2006; 1759(1-2): 99–107. [PubMed: 16494957]
19. Welch DR, Neri A, Nicolson GL. Comparison of ‘spontaneous’ and ‘experimental’ metastasis using rat 13762 mammary adenocarcinoma metastatic cell clones. Invasion Metastasis. 1983; 3(2): 65–80. [PubMed: 6677622]
20. Neri A, et al. Development and biologic properties of malignant cell sublines and clones of a spontaneously metastasizing rat mammary adenocarcinoma. J Natl Cancer Inst. 1982; 68(3):507–17. [PubMed: 6950180]
21. Roussos ET, B.M. Alford SK, Wyckoff JB, Gligorijevic B, Wang Y, Pozzuto M, Stobezki R, Goswami S, Segall JE, Lauffenburger DA, Bresnick AR, Gertler FB, Condeelis JS. Mena invasive (MenaINV) promotes multicellular streaming motility and transendothelial migration in a mouse model of breast cancer. Journal of Cell Science. 2011 In Press.
22. Wyckoff J, et al. A paracrine loop between tumor cells and macrophages is required for tumor cell migration in mammary tumors. Cancer Res. 2004; 64(19):7022–9. [PubMed: 15466195]
23. Wang W, et al. Single cell behavior in metastatic primary mammary tumors correlated with gene expression patterns revealed by molecular profiling. Cancer Res. 2002; 62(21):6278–88. [PubMed: 12414658]
24. Wyckoff, J., et al. High resolution multi-photon imaging of tumors in vivo, in Live Cell Imaging; A laboratory manual. Goldman, RD.; Swedlow, JR.; S., DL., editors. Cold Spring Harbor Laboratory Press; Cold Spring Harbor: 2010. p. 441-462.
25. Zipfel WR, Williams RM, Webb WW. Nonlinear magic: multiphoton microscopy in the biosciences. Nat Biotechnol. 2003; 21(11):1369–77. [PubMed: 14595365]
26. Gupta PK, Baloch ZW. Intraoperative and on-site cytopathology consultation: utilization, limitations, and value. Semin Diagn Pathol. 2002; 19(4):227–36. [PubMed: 12469790]
27. Mouneimne G, et al. Phospholipase C and cofilin are required for carcinoma cell directionality in response to EGF stimulation. J Cell Biol. 2004; 166(5):697–708. [PubMed: 15337778]
28. Loureiro JJ, et al. Critical roles of phosphorylation and actin binding motifs, but not the central proline-rich region, for Ena/vasodilator-stimulated phosphoprotein (VASP) function during cell migration. Mol Biol Cell. 2002; 13(7):2533–46. [PubMed: 12134088]

29. Lebrand C, et al. Critical role of Ena/VASP proteins for filopodia formation in neurons and in function downstream of netrin-1. Neuron. 2004; 42(1):37–49. [PubMed: 15066263]

30. Pino MS, et al. Human Mena+11a isoform serves as a marker of epithelial phenotype and sensitivity to epidermal growth factor receptor inhibition in human pancreatic cancer cell lines. Clin Cancer Res. 2008; 14(15):4943–50. [PubMed: 18676769]

31. Lin EY, et al. Progression to malignancy in the polyoma middle T oncoprotein mouse breast cancer model provides a reliable model for human diseases. Am J Pathol. 2003; 163(5):2113–26. [PubMed: 14578209]

32. Symmans WF, et al. Total RNA yield and microarray gene expression profiles from fine-needle aspiration biopsy and core-needle biopsy samples of breast carcinoma. Cancer. 2003; 97(12): 2960–71. [PubMed: 12784330]

33. Di Modugno F, et al. Human Mena protein, a serex-defined antigen overexpressed in breast cancer eliciting both humoral and CD8+ T-cell immune response. Int J Cancer. 2004; 109(6):909–18. [PubMed: 15027125]

34. Giampieri S, et al. Localized and reversible TGFbeta signalling switches breast cancer cells from cohesive to single cell motility. Nat Cell Biol. 2009

35. Zeineldin R, et al. Mesenchymal transformation in epithelial ovarian tumor cells expressing epidermal growth factor receptor variant III. Mol Carcinog. 2006; 45(11):851–60. [PubMed: 16788982]

36. Guy CT, Cardiff RD, Muller WJ. Induction of mammary tumors by expression of polyomavirus middle T oncogene: a transgenic mouse model for metastatic disease. Mol Cell Biol. 1992; 12(3): 954–61. [PubMed: 1312220]

37. Lin EY, et al. Colony-stimulating factor 1 promotes progression of mammary tumors to malignancy. J Exp Med. 2001; 193(6):727–40. [PubMed: 11257139]

38. Wyckoff JB, et al. A critical step in metastasis: in vivo analysis of intravasation at the primary tumor. Cancer Res. 2000; 60(9):2504–11. [PubMed: 10811132]

39. Wyckoff JB, et al. Direct visualization of macrophage-assisted tumor cell intravasation in mammary tumors. Cancer Res. 2007; 67(6):2649–56. [PubMed: 17363585]

40. Gertler FC, J. Metastasis:making tumor cells MENAcing. Trends Cell Biol. 2010 In press.

41. Wang W, et al. Tumor cells caught in the act of invading: their strategy for enhanced cell motility. Trends Cell Biol. 2005; 15(3):138–45. [PubMed: 15752977]

42. Wang W, et al. Coordinated regulation of pathways for enhanced cell motility and chemotaxis is conserved in rat and mouse mammary tumors. Cancer Res. 2007; 67(8):3505–11. [PubMed: 17440055]

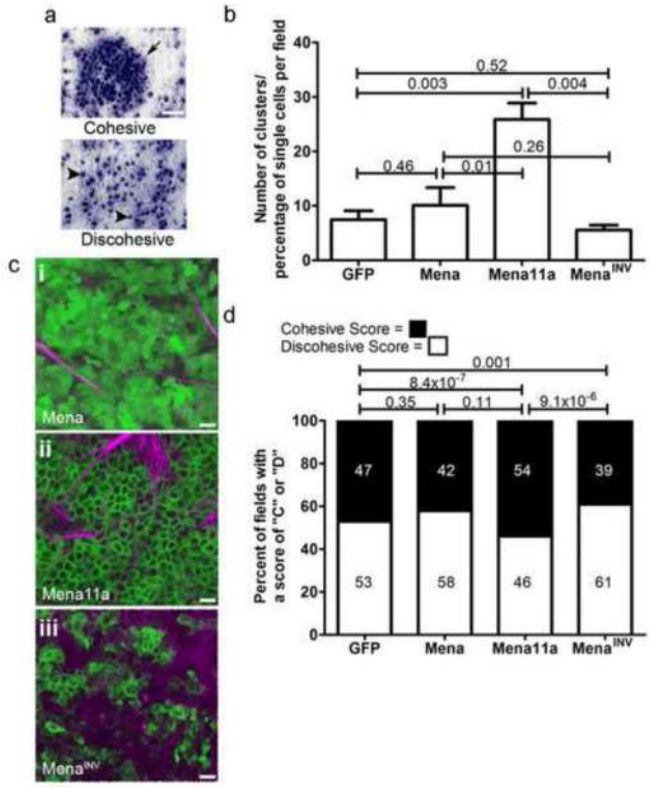

Figure 1. Mena11a promotes cohesive morphology while Mena^{INV} promotes discohesive morphology of the primary tumor *in vivo*

a. Representative Diff Quick stained smears of FNA samples from MTLn3-derived mammary tumors illustrating cohesive and discohesive cell patterns. Arrow= example of clusters scored in panel D. Arrowheads= single cells scored. Scale bars= 100 μm.

b. Ratio of number of clusters/ percentage of single cells. Each data set=10 smears/ tumor type shown. Error bars= SEM.

c. Multiphoton microscopy intra vital imaging (IVI) of MTLn3-EGFP-Mena, GFP-Mena11a and GFP-Mena^{INV} mammary tumors. Images represent one quadrant of a single field of view (512×512 pixels). Box i= GFP-Mena expressing tumor showing a mix of cohesive and discohesive morphology. Box ii= GFP-Mena11a expressing tumor showing cohesive morphology. Box iii= GFP-Mena^{INV} expressing tumor showing discohesive morphology. Scale bars= 50μm. Green= EGFP-fusion protein. Purple= collagen I second harmonic.

d. Quantification of primary tumor morphology from IVI. Scores were tallied and percentage of fields with each score was determined and represented in the bar graph. N= 15-25 fields/ cell type. “C” = cohesive, “D” = discohesive.

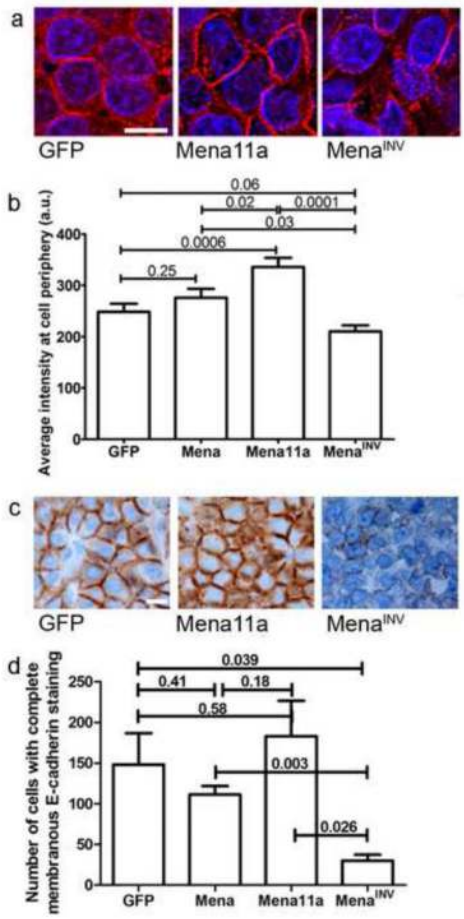

Figure 2. Mena11a promotes integrity of cell-cell contacts

a. GFP, Mena11a and Mena^{INV} mammary xenograft tumors stained for β-catenin. Red= β-catenin, Blue= DAPI. Scale bar= 25μm.

b. Average intensity of β-catenin determined at cell –cell contacts (2βm area around the cell periphery). N= 20 cells/ tumor type. Error bars= SEM

c. GFP, Mena11a and Mena^{INV} mammary xenograft tumors stained for E-cadherin. Brown= E-cadherin, Blue= hematoxylin staining. Scale bar= 25μm.

d. Average intensity of E-cadherin at cell-cell contacts. N= 30 high power fields (400x total magnification) per cell type. Error bars= SEM.

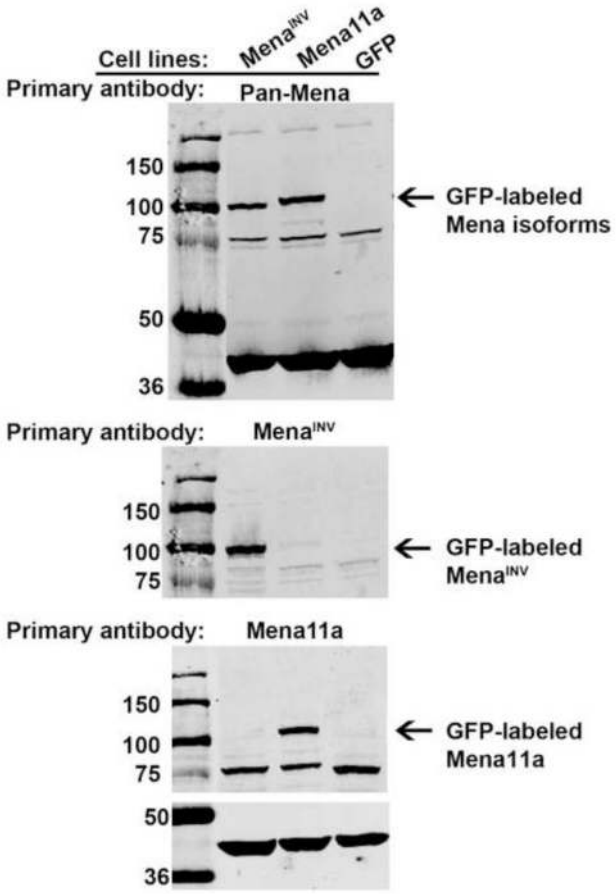

Figure 3. Western blot of Mena^{INV}, Mena11a and GFP cell lines for Mena, Mena11a and Mena^{INV}

Actin lanes shown in the top blot also apply to the middle blot (see methods section "western blots"). Note no changes in band intensity of bands in the molecular weight range 70-100 kDa where Mena isoforms migrate.

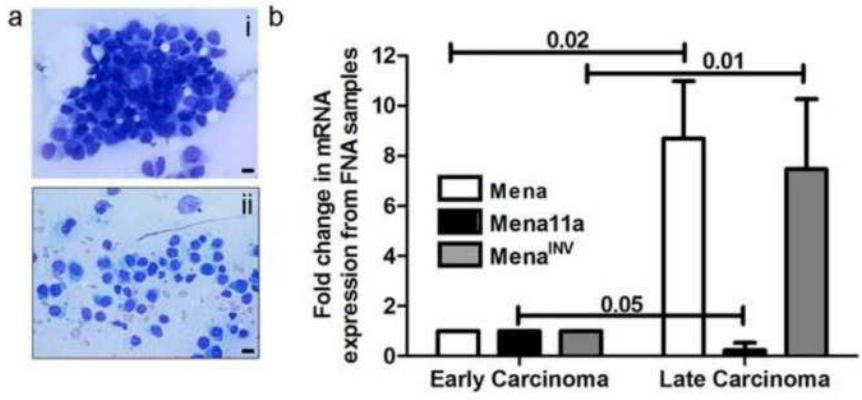

Figure 4. Mena^{INV} is associated with metastasis in PyMT mammary tumors

a. Smear pattern of early, non-metastatic (i) and late, metastatic (ii) invasive ductal carcinoma obtained from FNA samples of PyMT mouse mammary tumors.

b. Fold change of all Mena (pan-Mena), Mena^{INV} and Mena11a isoform mRNA expression in FNA samples from metastatic compared to non-metastatic PyMT carcinomas. The mRNA expression of Mena, Mena^{INV} and Mena11a in tumor cells collected by FNA was expressed as fold change in late carcinomas compared to early carcinomas. Error bars= SEM.

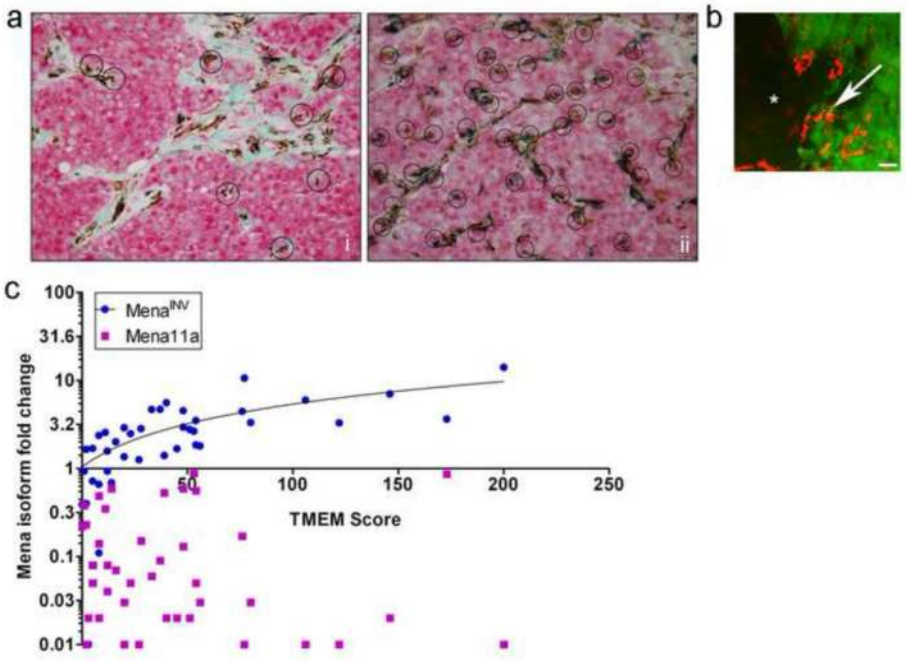

Figure 5. High TMEM count in human invasive ductal carcinomas of the breast is associated with increased fold change of Mena^{INV} expression

a. Examples of fields scored for TMEM (in circles), x400. Brown= macrophages. Blue= endothelial cells. Red= pan-Mena positive tumor cells.

b. TMEM—Multiphoton microscopy image of MTLn3 –EGFP-Mena^{INV} cells at sites of perivascular macrophages. Scale bar= 25μm. Green= MTLn3-EGFP-Mena^{INV}. Red= Texas-red dextran labeled macrophages. White arrow indicates location of TMEM where peri-vascular macrophages and Mena^{INV} expressing tumor cells are in direct contact with each other and the vessel wall. Asterisk indicates location of blood vessel.

c. Correlation of Mena^{INV} and Mena11a isoform mRNA fold change with TMEM count for 40 human invasive ductal carcinomas (Mena^{INV}: r= 0.78, p= 10^{-6}; Mena11a: r= −0.23, p= 0.14). Note the log scale of Y-axis.

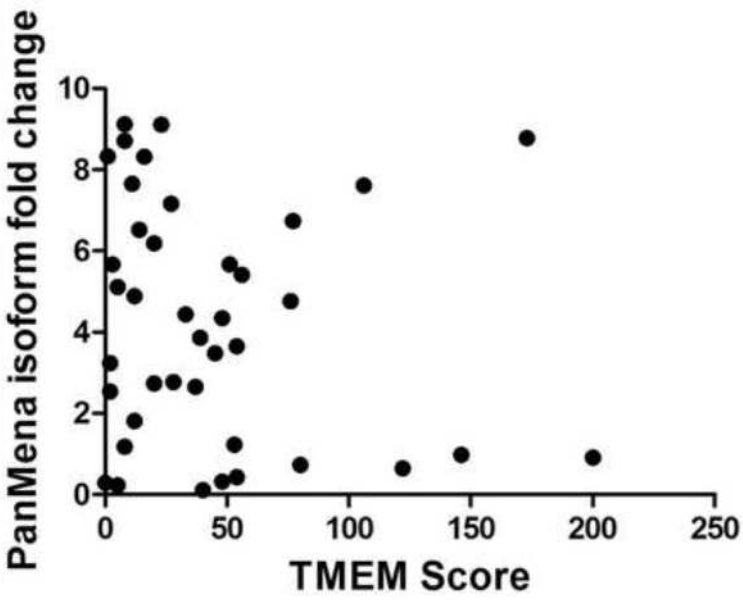

Figure 6. TMEM score does not correlate with the expression of pan-Mena mRNA in FNA samples

Lack of correlation of pan-Mena mRNA fold change with TMEM count for 40 human invasive ductal carcinomas ($r = -0.15$, $p = 0.37$).

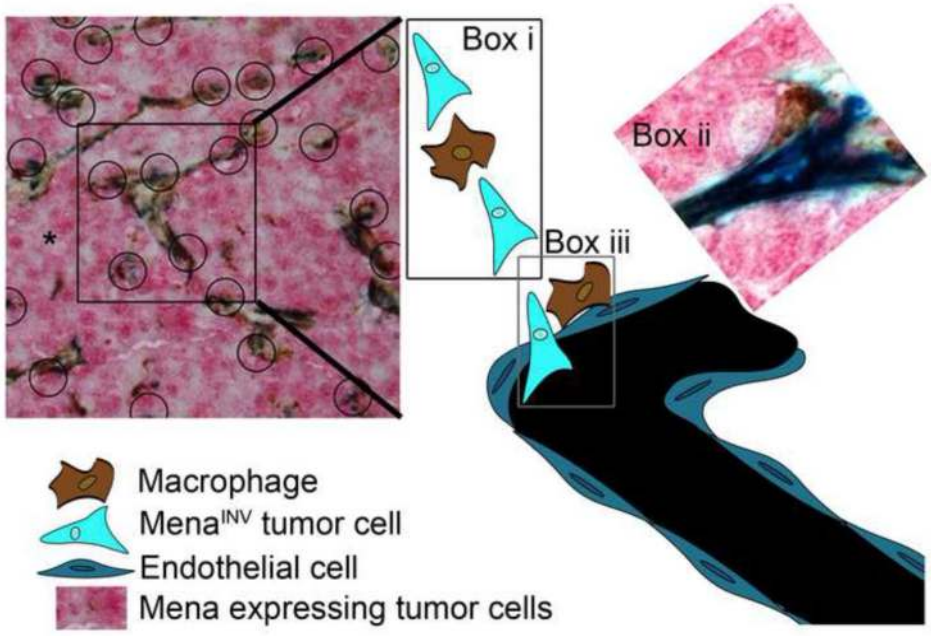

Figure 7. Tumor cell behavior in mammary tumors as related to Mena isoform expression

During tumor progression the spontaneous microenvironment-dependent decrease in Mena11a and increase in Mena^{INV} expression results in cell discohesion, migration towards blood vessels (Box i), formation of TMEM (circles in left box, and Box ii), transendothelial migration and intravasation (Box iii). Box ii is the IHC image of a TMEM as counted and schematized in Box iii. The black box (within the histology field) in the low magnification IHC image at the left represents the regions schematized in Boxes i and iii.

Table 1

Summary of Mena and TMEM values for tumors with different clinico-pathological variables

Median, 5th and 95th percentile of Mena^{INV}, Mena11a mRNA fold change, and TMEM counts for well (BR 3-5), moderately (BR 6 & 7) poorly (BR 8 & 9) differentiated invasive ductal carcinomas, tumors < 2cm, > 2 < 5 cm, > 5 cm, tumors with positive (+) and negative (−) estrogen (ER), progesterone (PR) and HER2/Neu receptor expression. Median is defined as a value that has exactly 50% of the data above and 50% below it. Likewise, 5th and 95th percentiles represent values that have 5% and 95%of the data below it respectively.

	Mena^{INV}	**Mena 11a**	**TMEM**
Tumor Characteristics:	Median *(5th, 95th percentile)*	Median *(5th, 95th percentile)*	Median *(5th, 95th percentile)*
BR 3, 4 & 5 N = 6	0.83 *(0.39, 2.47)*	0.06 *(0.02, 0.20)*	8.5 *(0.5, 26)*
BR 6 & 7 N = 14	2.38 *(0.50, 8.11)*	0.13 *(0.01, 0.64)*	39 *(1.7, 118)*
BR 8 & 9 N = 20	2.91 *(0.62, 5.65)*	0.05 *(0.01, 0.62)*	45 *(11.1, 175.7)*
< 2 cm N = 21	1.93 *(0.4, 6.0)*	0.07 *(0.01, 0.59)*	27 *(2, 146)*
> 2 < 5 cm N = 15	2.49 *(0.52, 6.49)*	0.08 *(0.01, 0.68)*	28 *(1.7, 76.4)*
> 5 cm N = 4	4.19 *(0.43, 12.81)*	0.02 *(0.01, 0.02)*	45.5 *(8.55, 177.65)*
LN + N = 15	2.71 *(0.08, 11.68)*	0.05 *(0.01, 0.68)*	40 *(2.7, 116)*
LN – N = 25	2.01 *(0.46, 5.74)*	0.06 *(0.01, 0.58)*	23 *(1.2, 141.2)*
ER + N = 30	2.75 *(0.39, 9.01)*	0.065 *(0.01, 0.74)*	38 *(1.45, 160.85)*
ER – N = 10	1.77 *(0.3, 3.83)*	0.06 *(0.01, 0.58)*	25 *(5.3, 52.65)*
PR + N = 24	2.75 *(0.39, 10.1)*	0.07 *(0.01, 0.56)*	32.5 *(1.2, 140)*
PR – N = 16	1.77 *(0.5, 4.92)*	0.06 *(0.01, 0.66)*	30 *(2.75, 134.75)*
HER2/Neu + N = 9	2.57 *(0.96, 4.63)*	0.09 *(0.02, 0.57)*	23 *(9.2, 67.2)*
HER2/Neu – N = 31	1.85 *(0.25, 8.83)*	0.05 *(0.01, 0.73)*	28 *(1.5, 159.5)*
Triple Negative N = 7	1.68 *(0.21, 4.12)*	0.02 *(0.01, 0.58)*	33 *(6.3, 53.1)*